JOURNAL OF SPACECRAFT AND ROCKETS
Vol. 33, No. 6, November–December 1996

Thrust Misalignments of Fixed-Nozzle Solid Rocket Motors

R. N. Knauber*
Lockheed Martin Vought Systems, Dallas, Texas 75265-0003

Major sources of thrust misalignments are described, and both ground test and flight data for several different upper stage solid rocket motors are presented. Special test data and flight data statistics are presented to show the known sources, such as 1) manufacturing mechanical tolerances, 2) motor case distortions and nozzle cant angles as a result of pressurization, 3) nonsymmetrical nozzle erosion, 4) transient gas flow phenomenon from internal ballistics, 5) center of mass radial offset as a result of static unbalance, and 6) static unbalance produced by propellant bore concentricity errors. Nozzle canting as a result of pressurization has been measured during hydrotest, and static firing was found to be the largest source of thrust misalignment in several composite case motors. Transient moments or side forces have been observed early in the burn period and during rapid thrust tailoff. A brief set of guidelines is presented for developing and testing new solid rocket designs to estimate the disturbing torque.

Nomenclature

I	= impulse, N-s
Pc	= chamber pressure, bar
T	= thrust, N
X	= body station, m
Z	= distance from centerline in pitch plane, m
ε	= thrust misalignment angle, deg
μ	= mean value
σ	= standard deviation
τ	= nondimensional lateral impulse

Subscripts

c.m.	= vehicle center of mass
P	= pitch plane
T	= thrust, or thrust application point (nozzle throat location)
Y	= yaw plane
ε	= thrust misalignment

Introduction

THE design of aerospace vehicles that use solid rocket motor propulsion requires accurate knowledge of the disturbing torque. These are used to define dynamic forcing functions and error sources for unguided missiles and control requirements for guided vehicles. The side forces and pitching and yawing moments produced by the solid rocket motor are generally described as thrust misalignments. There are few data and design information available in the open literature on this subject. The intent of this paper is to help fill the void.

Strictly speaking, thrust misalignment, or malalignment, is the thrust vector offset from the centerline both translational (lack of concentricity) and angular (lack of parallelism) (Fig. 1). The translational as well as the angular terms result in pitch and yaw torque about the vehicle center of mass. For purposes of this paper, thrust misalignment will be defined as the equivalent angular misalignment of the thrust vector acting at the location of the nozzle throat, which accounts for all of the pitching and yawing torque about a vehicle center of mass. Most transverse moments produced by solid rocket motors result from side forces generated in the nozzle.

The presented data are from accumulation of design, test, and flight data for many of the fixed-nozzle solid rocket motors used on the NASA solid controlled orbital and utility test vehicle (SCOUT) launch vehicle and the U.S. Air Force air-launched antisatellite vehicle (AL-ASAT) upper stage. The SCOUT is a four-stage solid propellant small satellite launch vehicle (Fig. 2). From 1960 to 1994 this vehicle used at least two or three motor designs for each of the four stages. Disturbing torques were extracted from flight data for most of the 118 flights. Since the upper three stages are exoatmospheric, there are no aerodynamic moments to obscure the disturbing forces or moments contributed by the solid rocket motor. A summary of the motor characteristics is presented in Table 1.

Special hydrotests and development and qualification static firings were conducted for both the SCOUT and AL-ASAT from which several distinct sources of the side forces and thrust misalignments were extracted.

Causes of Thrust Misalignment

Most upper stage solid rocket motors are designed to have less than a 0.25-deg thrust misalignment. Some motors have been developed to keep the three sigma thrust misalignment below 0.15 deg by maintaining very tight tolerances on concentricity and parallelism of nozzle and interstage mounting flanges, designing motor cases to relatively low values of strain, and designing nozzles for uniform low-erosion characteristics. Thrust misalignments can include pseudo-steady-state, slowly varying, and highly transient phenomena.

Pseudo-Steady-State Thrust Misalignments: Type A

Steady-state thrust misalignments are mostly a result of tolerances on manufacturing and assembly of the rocket motor and nozzle. The

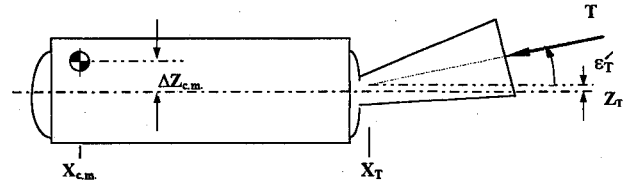

Actual disturbing moment

$$M_{\text{c.m.}} = T(X_T - X_{\text{c.m.}})(\varepsilon_T'/57.3) + T(\Delta Z_{\text{c.m.}} - Z_T)$$

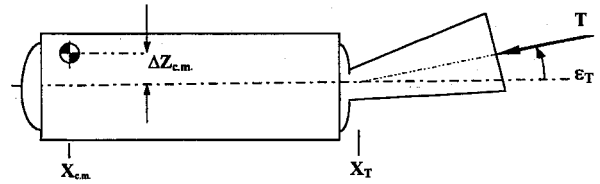

Effective thrust misalignment

$$\varepsilon_T = \varepsilon_T' + [57.3(\Delta Z_{\text{c.m.}} - Z_T)/(X_T - X_{\text{c.m.}})]$$

Fig. 1 Effective thrust misalignment definition.

Presented as Paper 95-2874 at the AIAA/ASME/SAE/ASEE 31st Joint Propulsion Conference, San Diego, CA, July 10–12, 1995; received Aug. 23, 1995; revision received June 21, 1996; accepted for publication July 9, 1996.

*Consulting Engineer, Flight Dynamics and Aerodynamics, Mail Stop EM-55. Senior Member AIAA.

Table 1 SCOUT solid rocket motor data

Motor	Diam., mm	Length, mm	Prop., kg	Burn, s	Web, s	T_{max}, kN	Pc, bar	Case material	Sample size
Algol III	1143	9093	12,716	85	58	756	55	Steel	38
Castor I	787	6198	3,379	40	27	267	38	Steel	39
Castor II	787	6248	3,751	41	38	311	41	Steel	78
X-254	762	2718	1,021	41	39	62	28	Glass	8
ABL X-259	762	2718	1,134	32	29	107	24	S glass	24
Bacch. X-259	762	2718	1,134	32	29	107	24	E glass	32
HP-X-259	762	2718	1,134	27	24	147	41	E glass	3
Star 31	762	2718	1,286	48	45	93	62	Kevlar	12
FW-4S	559	1549	272	34	29	29	54	Glass	12
Star 20A	500	1486	272	32	28	31	57	Glass	12
Star 20B	503	1486	272	34	31	29	54	Glass	3

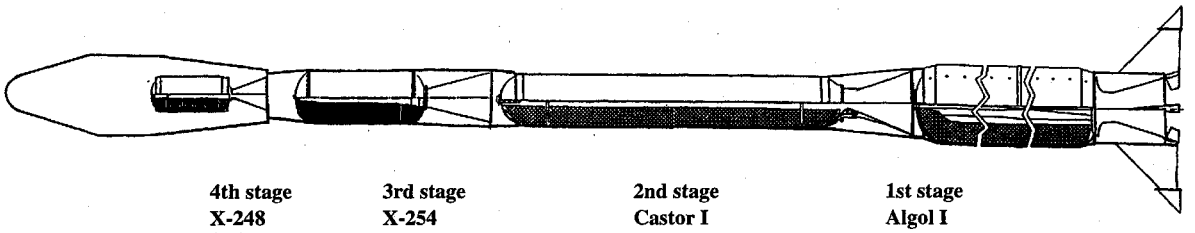

Fig. 2 SCOUT solid rocket motors.

most sensitive component is the nozzle angular alignment. Nozzles can be manufactured and installed with tolerances of less than 0.05-deg three sigma. The nozzle angle tolerance buildup includes 1) motor case aft nozzle flange parallelism and concentricity as machined, 2) nozzle and attachment flange parallelism and concentricity as machined, 3) changes in case shape as a result of casting, and 4) changes in case and nozzle angle as a result of creep in storage.

Slowly Varying Thrust Misalignments: Type B

Thrust misalignments that change relatively slowly with time are categorized as type B. Sources include 1) changes in motor case and nozzle angle as a result of distortions under slowly changing chamber pressure and 2) gas flow misalignment as a result of unsymmetric burning and nozzle erosion.

Rapid Transient Thrust Misalignments: Type C

These are relatively shortly lived transients or abrupt changes in thrust misalignment in a very short period of time. Sources include 1) unsymmetric strain changes in aft dome during rapid pressurization and decay, 2) erratic changes as a result of low-level acoustic instabilities, and 3) nozzle throat chipping as a result of ejection of igniter.

Ignition Transients: Type D

Ignition transient side forces as a result of the unsymmetric startup of gas flow and nozzle flow can produce very large thrust misalignment angles before the motor achieves full operating pressure. Being short in duration (15–30 ms) these excite vehicle structural modes and cause "tipoff" angular rates. These are important in uncontrolled spin stabilized missile applications. Data have been accumulated from SCOUT fourth-stage ignition analyses.

Static Unbalance as a Result of Bore Concentricity: Type E

If a motor is cast with the bore offset from its centerline, static unbalance increases with burning time. The rocket center of mass radial offset increases by an order of magnitude between ignition and web time. The thrust vector couples with the center of mass offset to produce a disturbing torque.

Static Unbalance and Rocket Motor to Vehicle Alignment: Type F

Vehicle static unbalance is not truly a thrust misalignment attributable to the rocket motor but is a result of vehicle alignment tolerances and mass dissymmetry. With care this can become an insignificant contributor to the disturbing moments acting on a vehicle. The alignment between the rocket and an upper stage or payload behaves like a vehicle inert weight static unbalance. As the rocket burns off propellant, the vehicle center of mass travels further from the centerline to effectively increase the apparent thrust misalignment.

Data Obtained from Flight and Special Test

There is not much widely disseminated data that provide actual measurements of all of the preceding terms. Overall thrust misalignment data are obtained from flight data and some special testing. Most of the sources presented in this paper are from detailed thrust misalignment data extracted from SCOUT flight data and include time histories of the pitch and yaw components.[1] (Many other SCOUT documents that are not widely disseminated were used in this paper.) Special ground testing measurements were also made for the AL-ASAT.[2] Other flight data have also appeared in the open literature for the Burner II vehicle[3] and Strypi IX vehicles.[4] Flandro[5] published one of the early works on disturbing force data relative to internal acoustic phenomena.

The SCOUT X-259, Star 31, and AL-ASAT Star 20B motors were developed with systematic measurement and testing to isolate the sources of thrust misalignment and side forces. After manufacturing and assembly, the static alignment of the motor case and nozzle was measured. Changes in motor case and nozzle deflections, as a result of pressurization, were measured both in hydrotest and static firing using deflectometers and strain gauges. Dynamic changes in thrust misalignment as a result of internal ballistic phenomena and unsymmetric nozzle erosion were deduced from the measured side forces and moments during static firing.

Flight Data Examples

The first three stages of the NASA SCOUT launch vehicle were three-axis stabilized. The fourth stage was spin stabilized at 2.5–3 rps (revolutions per second). The upper three stages were exoatmospheric. Postflight analyses for each flight included extraction of pitch, yaw, and roll disturbing torque and effective thrust misalignment. Analyses of telemetry data allowed calculation of effective thrust misalignments to within 0.005-deg accuracy.

Castor I

The Thiokol Castor I motor thrust time history and effective pitch and yaw components of thrust misalignment indicate a bias in the pitch-up direction (Fig. 3). Some possibilities include effects of horizontal assembly and slump of motor grain as a result of horizontal storage (stored with pitch plane vertical).

A transient type C disturbance has occurred on 3 of the 39 flights. Thrust misalignment rose significantly 3–4 s before web time (Fig. 4). No other anomaly was detected in motor performance on these flights. The cause of the observed change is not totally understood. It may be related to the internal gas flow. This motor has a five point star grain, which results in five longitudinal slivers of burning propellant during the long tailoff period.

Castor II

The Thiokol Castor II motor has the same external envelope as the Castor I. It packs more propellant by using a smaller cylindrical smooth bore with two end radial slots (Fig. 5). This motor was flown on 79 SCOUT flights. The statistical distribution of thrust misalignment indicates 0.1-deg pitch-up bias.

The Castor II also produced a type C pitch-up transient at ignition. One second after ignition the three sigma peak value is almost 0.5 deg. The cause is not known. Like other SCOUT motors the Castor II was always stored horizontally with the pitch plane vertical.

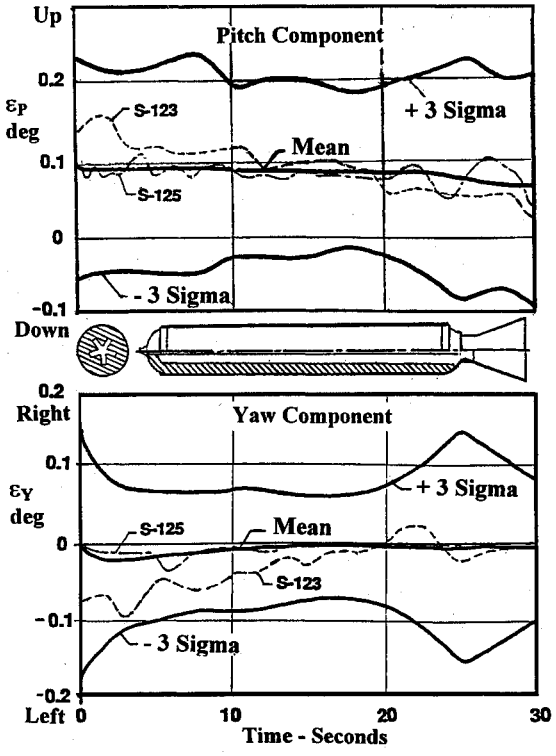

Fig. 3 Castor I flight statistics.

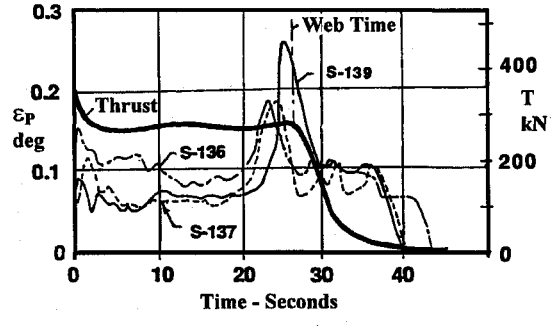

Fig. 4 Castor I web time transient.

Table 2 Static nozzle misalignment statistics for X-259 motors

	Mean	Standard deviation	Tolerance
Angle			
Pitch, deg	0.00376	0.00965	0.057
Yaw, deg	0.00270	0.00829	0.057
Radial offset, mm	0.203	0.107	0.38

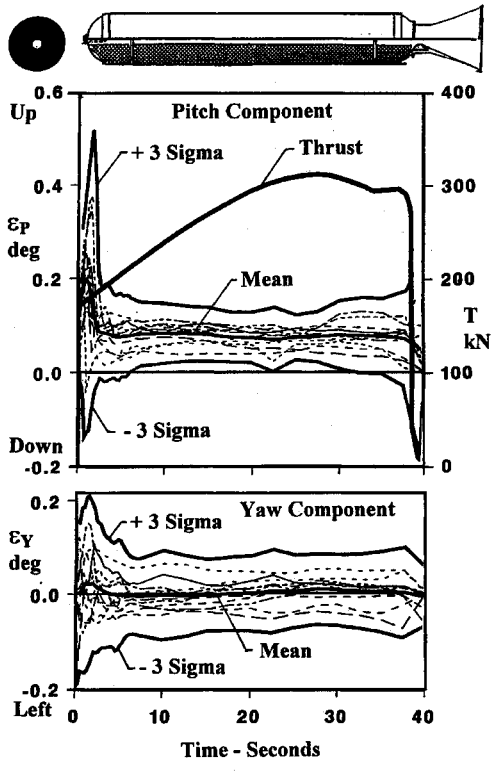

Fig. 5 Castor II flight statistics.

X-259

The Hercules X-259 was the SCOUT third-stage motor on more than 90 flights from 1961 through 1983. Although nozzle alignments were not measured on all SCOUT motors, X-259 manufacturing tolerance measurements were available from another program. After casting and nozzle installation, motors were mapped for nozzle alignment. Static nozzle misalignment statistics from 57 X-259 motors are given in Table 2.

Several modifications to the X-259 motor were flown on SCOUT. Most configurations burned with low chamber pressure (24 bar, 350 psi). The filament wound motor cases were changed in 1966 from an E glass to S-901 glass material. The modulus of the latter material increased the case burst strength from 46 to 76 bar. There was no change in nozzle, propellant grain, or other characteristics. Thus, the thrust time history was unchanged. The extracted thrust misalignment showed a statistically significant reduction in the standard deviation after the case was strengthened (Fig. 6). The reduction in the standard deviation of thrust misalignment is inversely proportional to the burst strength of the case. Subsequent special hydrotesting indicated that the nozzle and skirt movements under pressure were the most significant source of thrust misalignment for the X-259 (Fig. 7).

A later modification of this motor, HP-X-259, almost doubled the chamber pressure to 42 bar by introducing a nozzle with a smaller throat diameter. The motor case and propellant were unchanged. The thrust misalignment increased proportionately. Special hydrotesting of the motor case included mapping the motor case with a closed tube nozzle simulator. Distortions of the motor case and nozzle cant were determined as a function of pressure for three motor cases. One case showed the most significant nozzle deflection during the

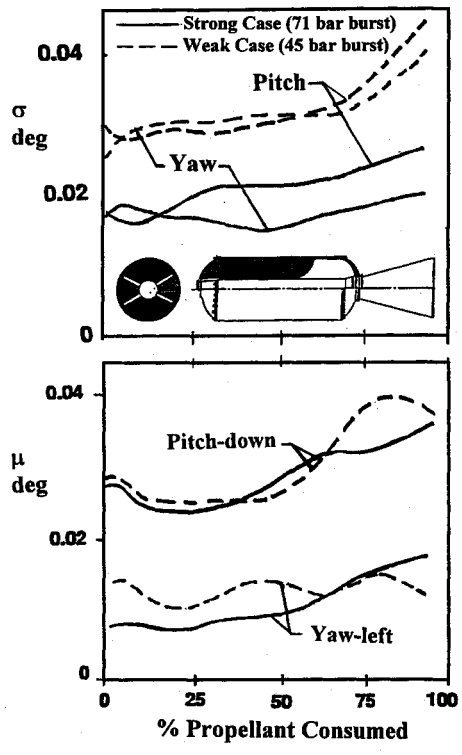

Fig. 6 X-259 flight statistics.

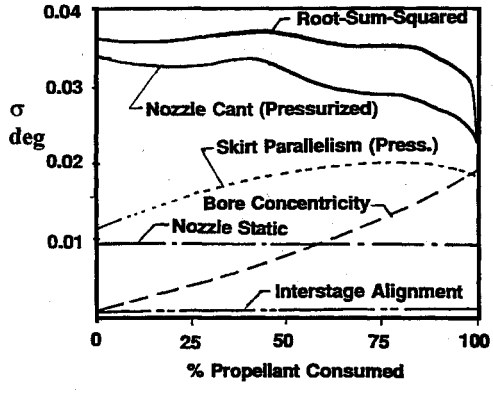

Fig. 7 X-259 thrust misalignment sources: thrust misalignment standard deviation.

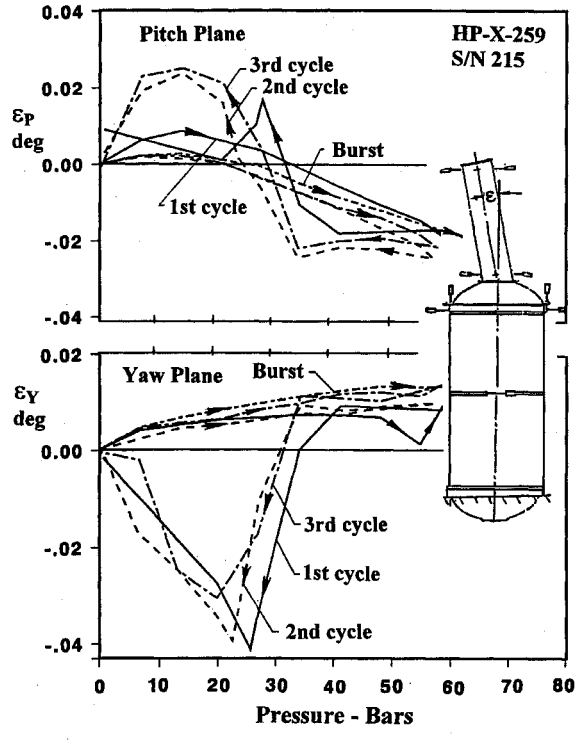

Fig. 8 HP-X-259 motor case hydrotest data.

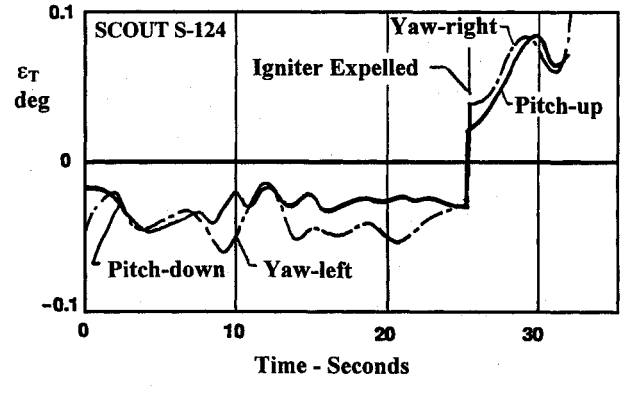

Fig. 9 X-259 flight S-124 nozzle chipping.

depressurization phase (Fig. 8). This case repeated this behavior for three cycles.

The X-259 used a head end igniter, which was insulated only on later flights. On all earlier flights the igniter would burn off and eject through the nozzle about 70% into the burn. On one occasion, flight S-124, simultaneous with the igniter ejection (observed by a chamber pressure high-frequency pulse and vehicle vibration) the thrust misalignment instantaneously changed quadrants by about 180 deg (Fig. 9). On later flights a special insulating boot was used on the igniter to keep it from burning off and being ejected.

Star 31 (Antares IIIA)

This Thiokol motor was developed as a higher-performance, high-reliability motor for the SCOUT third-stage application. A detailed development and test program included special hydrotesting, development and altitude qualification static firings. This Kevlar® case motor was designed to a side force specification to allow use of the existing SCOUT reaction control system. Statistical data predictions based on development and qualification test data were well within the specifications. Flight data statistics from the 13 flights showed a three sigma value less than 0.15 deg (Fig. 10).

Static unbalance as a result of bore concentricity tolerances can become significant as a motor burns. The Star 31 specification tolerance on this parameter was 1.27 mm (0.05 in.) maximum. Fully loaded, this tolerance causes less than 0.12 kg-m (10 in.-lbm) static unbalance (Fig. 11). As the propellant burns around the offset bore, the static unbalance increases by an order of magnitude. The center of mass offset increases by an even greater factor since the vehicle weight is being reduced as propellant burns. If not properly controlled, this can cause significant type E disturbances.

Highly transient type C disturbances have occurred during tailoff of composite case motors. The Star 31 has an abrupt tailoff. On the first flight, S-203, a transient disturbance during tailoff created 590 N-m (435 ft-lbf) of vehicle pitch-up moment (Fig. 10). The equivalent thrust misalignment was 0.28 deg. This is usually not of concern on a controlled vehicle because of the very short transient time. However, such disturbances can be critical in spin stabilized applications.

Flight data statistics indicate a pitch plane bias and a larger standard deviation in the pitch plane than in the yaw plane (Fig. 10). Pitch plane biased thrust misalignment may be related to motor long-term horizontal storage and the horizontal assembly of the vehicle. Recertification of several motors that were in storage for 10 years indicated no significant degradation or slump of the case or the bore. There was less than 0.02 deg of nozzle cant change after 10 years storage time and no measurable bore concentricity shift. When these motors flew, there was not a strong correlation of preflight measured nozzle cant and the observed in-flight disturbance.

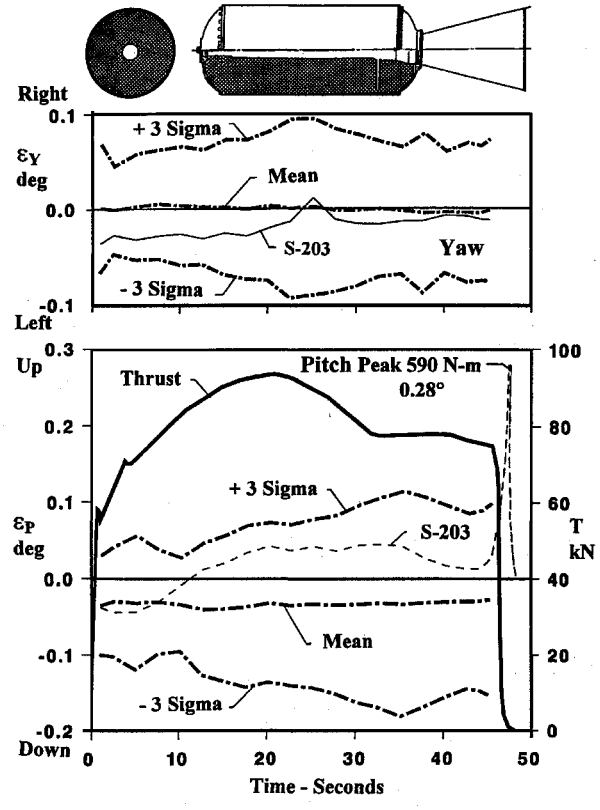

Fig. 10 Star 31 flight data statistics.

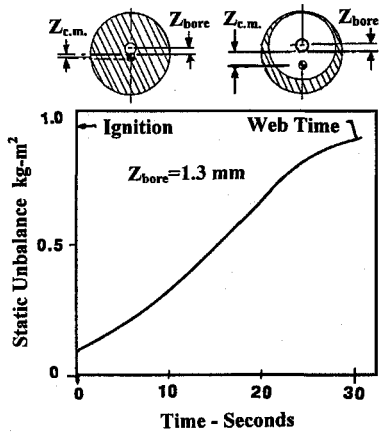

Fig. 11 Star 31 static unbalance: bore concentricity.

Star 20A (Altair IIIA)

This Thiokol motor has been flown as a spin stabilized orbital injection motor on 34 SCOUT flights. Flight data statistics of the thrust misalignment are presented in Fig. 12. This orbital injection motor spins at 2.5 rps and is ignited after a separation distance of at least three body diameters. A type C ignition transient nozzle side force, not shown in Fig. 12, causes a tipoff rate change to the vehicle. This is separate from the tipoff rates that occur 4 s earlier at separation. Bowyer et al.[6] associate the transient with an oblique starting shock traveling down the nozzle length at ignition. The lateral impulse acting on the nozzle exit cone has been taken from instrumented flights. The mean value is 11.4 N-s (2.56 lbf-s) with a standard deviation of 4.9 N-s (1.1 lbf-s). Based on observed structural and rigid body motions, the lateral forcing function can be approximated as a half-sine pulse having a duration of about 22 ms before the motor achieves full operating chamber pressure. This type C transient could be normalized by the peak thrust after ignition to provide a time constant factor for general application to other altitude firings of motors for which there is no database, i.e.,

$$\tau_I = \frac{I_{\text{side}}}{T_{\max}} \tag{1}$$

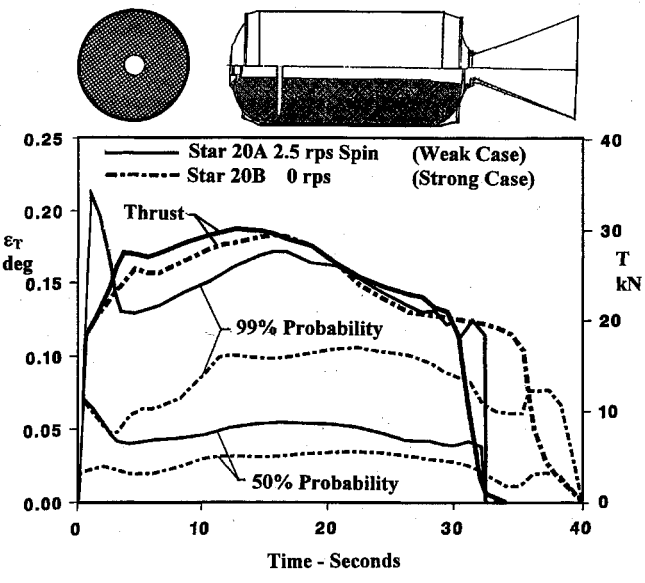

Fig. 12 Star 20 statistics.

A mean plus three sigma value for this factor based on the Star 20A motor is

$$\tau_I = \frac{26.06N - s}{17,800N} = 0.00146\,\text{s} \tag{2}$$

An order of magnitude estimate of lateral impulse for an untested motor design could be given by

$$I_{\text{side}} \cong \tau_I T_{\max} \tag{3}$$

This impulse would be spread over a 22-ms duration half-sine pulse to generate a lateral forcing function for ignition loads analyses.

Star 20B

The successful Air Force AL-ASAT used the Thiokol Star 20B for the second-stage rocket motor. This motor was a modification of the Star 20A. Load environments for this application required a considerably stronger motor case than the Star 20A. Hydrotesting and subsequent qualification testing at the Arnold Engineering Development Center showed a decrease in the standard deviation of thrust misalignment of nearly 50% from the Star 20A as a result of the stronger and lower strain motor case design; see Fig. 12. The standard deviation of thrust misalignment is approximately inversely proportional to the case strength. This result is very similar to the experience with the X-259 motor.

Transients During Tailoff

During thrust decay of a solid rocket motor there are several factors that can induce transient moments and thrust misalignments including 1) pressure vessel relaxation dissymmetries and 2) large gas flow misalignment as a result of nonsymmetric propellant sliver burnout. In many cases, the thrust misalignment angle is considerably larger during this transient than during the steady-state burn phase of a rocket motor as shown for the Castor I and Star 31; see Figs. 4 and 10.

On many of the SCOUT flights, a transient in the effective thrust misalignment angle is observed during tailoff. These transients are short lived and do not impose stringent problems for a robust reaction control system. They are of concern for spin stabilized systems. The more severe cases can produce up to 0.5 deg of thrust misalignment peak during this transient and reverse direction during the short tailoff time. Transients observed in hydrotests (Fig. 8) show that at least part of this phenomenon can be a result of erratic nozzle cant during rapid aft dome strain relaxation.

Tailoff transients have also been observed on larger motors with longer tailoff times. The United Technologies Corporation Algol IIIA SCOUT first-stage motor is a steel case design having a fixed nozzle. On 25% of the flights a pitch-up thrust misalignment transient has been observed starting with web time and lasting up to 12 s

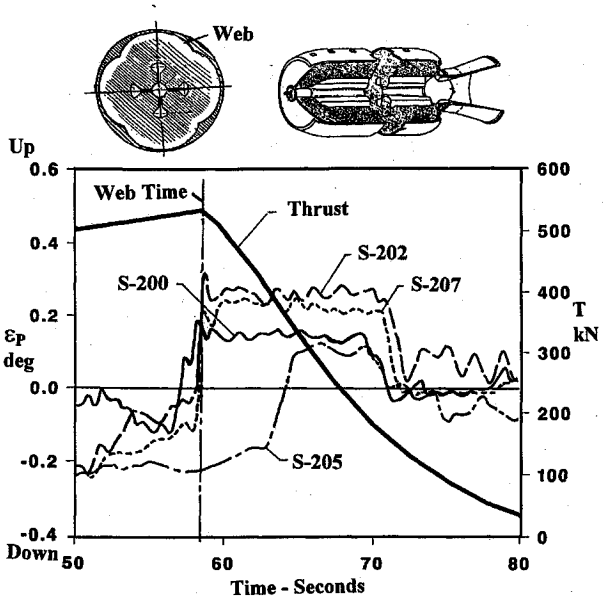

Fig. 13 Algol III web time transient.

of the 25-s tailoff period. The thrust misalignment change, as high as 0.35 deg, has been observed (Fig. 13). The transient on this motor is a sudden shift in and out with varying duration, a square wave pattern.

Guidelines for New Vehicle Development

A few guidelines are recommended for flight dynamics, control system, and propulsion engineers on new vehicle designs. These include the following: 1) Review the types of phenomena that have occurred in the past relative to solid rocket motor induced side forces and torque. This paper should provide a starting place. 2) Evaluate the significance of the disturbances to the vehicle control design and dynamics. If the effects are significant, perform the remaining steps. 3) Estimate the statistical magnitude of each source of disturbance and determine an error budget for specifications imposed on the rocket motor, vehicle manufacturing, and assembly tolerances. 4) Prepare a test plan that defines sufficient detail to measure and to verify the more significant sources of side forces and moments during the development and qualification phases of the solid rocket motor. 5) Measure manufactured hardware tolerances for the development and qualification hardware. 6) Measure motor case distortions and simulated nozzle movement under pressure during hydrotesting. These should include those cases destined for development and qualification ground firing. 7) Measure mating surfaces and nozzle concentricity and parallelism of all development and qualification rounds before and after propellant loading. 8) Measure the static unbalance and bore concentricity of the development and qualification rounds. 9) Trace "as manufactured" motor alignments of development and qualification rounds to be used for static firing tests and include these data in the mapping for static firing stand alignments and calibrations. 10) Measure changes in motor case and nozzle cant angles during development and qualification static firings. Also measure side forces and moments during these tests. 11) Carefully reduce test data accounting for measured and expected sources of side forces and moments. The residuals can be attributed to gas flow asymmetries and other unmeasurable phenomena. 12) Extract disturbances from early flights or flight tests for correlation with development cycle statistics.

If all sources of thrust misalignment are appropriately accounted for in the ground measurements, then predicted statistics for disturbances should yield a conservative estimate when compared with flight test data. The conservatism results from measurement errors associated with the multiplicity of ground measurement and test data sources needed to predict total disturbance levels. Some or all of the tolerance measurements performed during development and qualification may be continued during the production phase if they are critical to the vehicle flight success.

Conclusions

There are many sources of disturbing forces and moments produced by solid rocket motors. Many of these can be significantly larger than the engineering drawing tolerance stackup of mechanical alignments. The more significant sources are nozzle movement and motor case distortions as a result of pressurization, unsymmetric internal and nozzle gas flow, and, in some cases, poor control of manufacturing tolerances. Flight data and special ground test data presented herein can be used for first-order approximation of disturbances for flight dynamics and control estimates for new vehicle designs. The methods of testing to mitigate risk in new designs should include a well-defined plan and execution of 1) analyses, 2) ground test measurements, and 3) flight data correlation.

References

[1]Black, C. E., Barraza, A., Kreiter, G. W., and SCOUT Engineering, "SCOUT Flight Data Historical Summary," Lockheed Martin Vought Systems, Rept. 3-34100/9R-12, Dallas, TX, Vol. 1, July 1973; Vol. 2, Sec. 4.0, Rev. A, Feb. 1990.

[2]Knauber, R. N., "ASAT Upper Stage Motor AEDC Side Force and Roll Torque Test Data," Lockheed Martin Vought Systems, Rept. 211-07-AG-30202, Dallas, TX, June 1983.

[3]Dionne, E. R., and Kosmann, W. J., "Characterization of the Non-Axial Thrust Generated By Large Solid Propellant Rocket Motors in Three Axis Stabilized Ascent," AIAA Paper 78-1076, July 1978.

[4]Edmunds, R. S., "In-Flight Motor Torque Estimates for the Second-Stage Strypi IX Launch Vehicle," AIAA Paper 88-3347, July 1988.

[5]Flandro, G. A., "Roll Torque and Normal Force Generation in Acoustically Unstable Rocket Motors," *AIAA Journal*, Vol. 2, No. 7, 1964, pp. 1303–1306.

[6]Bowyer, J. M., Kreiter, G. W., and Petersen, R. E., "An Investigation of the Side Force That is Sometimes Observed in Rocket Motor Start-Up," AIAA Paper 78-1045, July 1978.

J. C. Adams
Associate Editor